Exploitation of host chemokine signalling by pathogenic mycobacteria

Torraca, V.

Chapter 4

Disruption of chemotactic signalling primes the lysosomal function of macrophages to counteract mycobacterial parasitism

Vincenzo Torraca, Eveline in't Veld and Annemarie H. Meijer

Institute of Biology, Leiden University, The Netherlands

Manuscript in preparation

Chapter 4

Disruption of chemotactic signalling primes the lysosomal function of macrophages to counteract mycobacterial parasitism

Vincenzo Torraca, Eveline in't Veld and Annemarie H. Meijer

Institute of Biology, Leiden University, The Netherlands

Chemokine receptors and their cognate ligands are essential host factors that control leukocyte migration and inflammation. We previously described that disruption of the CXCR3-CXCL11 receptor-ligand signalling axis in zebrafish carrying a *cxcr3.2* null mutation attenuates macrophage motility and recruitment to infectious foci. Importantly, these defects in macrophage function are associated with increased resistance to *Mycobacterium marinum*, a zebrafish pathogen widely used to study tuberculosis pathogenesis and macrophage parasitism. Here we revealed by RNA deep sequencing that lysosomal genes are significantly upregulated in sorted macrophages from the *cxcr3.2* mutant. *In vivo* assays subsequently showed increased lysosomal content, augmented acidification of phagosomes containing bacteria, and increased microbicidal capacity in *cxcr3.2* mutants. Tracking of macrophage lysosomes *in vivo* revealed that these organelles mostly localise at the leading edge of motile cells. We show that maintenance of polarised lysosomes during cell migration requires a functional *cxcr3.2* gene, suggesting that Cxcr3.2-dependent signalling affects lysosomal content by sustaining lysosomal exocytosis. Strikingly, macrophages respond to *M. marinum* infection by upregulation of Cxcl11aa, the cognate ligand of Cxcr3.2, in a Myd88/Nfκb dependent manner. This suggests that mycobacteria take advantage of the Myd88-immune signalling to sustain *cxcl11aa* expression, manipulate the Cxcr3.2 pathway and ultimately control the lysosomal content of the parasitised cell. Taken together, these data reveal a molecular pathway that links macrophage chemotaxis to lysosomal function. In the absence of this pathway, macrophages are primed for antimicrobial defence by enhanced lysosomal gene expression and microbicidal capacity. In turn, exploitation of this circuit by intracellular parasites could lead to a more permissive replicative niche where the infection is initiated.

GRAPHICAL ABSTRACT

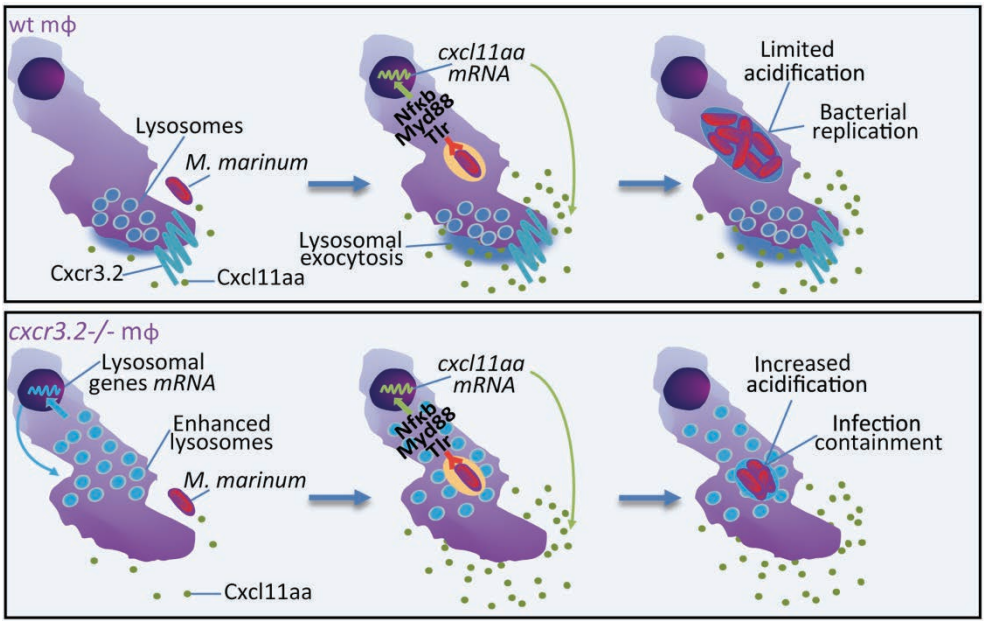

Chemokine signalling via Cxcr3.2-Cxcl11aa controls the distribution of lysosomes in macrophages and regulates coordinated transcription of lysosomal genes. Cxcr3.2 signalling maintains cell polarisation and localisation of lysosomes to the leading edge of the cell, where lysosome exocytosis is thought to facilitate cell migration. Deficiency of *cxcr3.2* reduces random migration as well as lysosome polarisation and results in upregulation of lysosomal genes. As a consequence, *cxcr3.2* mutants have a better capability to counteract bacterial replication, due to their enhanced lysosomal function. *Mycobacterium marinum* can induce high upregulation of *cxcl11aa* in infected macrophages via TLR/Myd88-mediated recognition. Exploitation of this autocrine system could benefit the pathogen as it triggers the chemokine/lysosome circuit which would further suppress lysosomal function and generate a more permissive environment for bacterial replication.

INTRODUCTION

Chemokines are a class of endogenous peptides with chemoattractive properties, produced at sites of infection and inflammation to induce the recruitment of leukocytes[1]. These motogenic mediators can control both random and directional motility, also known as chemokinesis and chemotaxis, respectively[2]. Activation of chemokine receptors transduces a complex cascade of signals that results in cell polarisation[3], characterised by an asymmetrical shape of the cell body and by an unequal distribution of the cytosolic contents, including organelles such as mitochondria and lysosomes[4,5]. To efficiently migrate into inflamed tissues, macrophages must acquire and maintain these spatial and functional asymmetries, and therefore expression of chemokine receptors on their plasma membrane is critical for their function.

In both mammalian and teleost species, macrophages express the CXC-motif chemokine receptor CXCR3[6,7], which, via its cognate ligands CXCL9-10-11, has been shown to exert remarkably pleiotropic functions on these cells. These activities not only include a direct control of macrophage trafficking to localised infectious/inflamed foci[8,9,10,11] but also their capability to activate differential functional programs in response to microenvironmental signals. This is well exemplified, for instance, by the impairment of macrophage-mediated vascular remodelling[12], the skewing of M1/M2 differentiation[13] and the increased clearance of pathological protein aggregates[14] or steatotic lipid inclusions[15] in CXCR3-deficient conditions.

Despite that much effort has been made to elucidate the sequence of events activated by the transduction of chemokine signals, we are only beginning to understand the transcriptional and subcellular effects of the chemokine-mediated cell polarisation and the implications of these effects on the immune function of leukocytes. Additionally, our current understanding of chemokine responses derives mostly from studies performed *in vitro*. Here we used the zebrafish model and RNA-sequencing analysis of sorted macrophages to elucidate the downstream targets affected by chemokine signalling *in vivo*. Using the mutant line of the chemokine receptor *cxcr3.2* (a functional homologue of the mammalian CXCR3), we show that the disruption of CXCR3-CXCL11 signalling results in transcriptional upregulation of lysosomal genes and primes the microbicidal function of macrophages. This transcriptional signature is linked with reduced macrophage motility in *cxcr3.2* mutants and attenuated susceptibility to the fish and macrophage pathogen *Mycobacterium marinum* (*Mm*)[10].

Our findings provide a novel addition to the current understanding of the leukocyte chemotactic process, since it was recently shown that lysosome delivery to the leading edge of motile cells and their local exocytosis is critical to permit chemotactic migration and to fuel lipid endomembranes to the lamellipodium. Strikingly, we found that mycobacterial immune recognition by Myd88-dependent signalling can induce large autocrine induction of Cxcl11aa, the cognate ligand of Cxcr3.2. Therefore, this immune recognition/chemokine/lysosome circuit might represent an unexpected macrophage-autonomous mechanism of pathogen virulence. Mycobacterial parasitism may exploit the chemokine signalling to dissipate lysosomal function and maintain a macrophage phenotype that is more permissive for the establishment of the infection.

RESULTS

Macrophage chemotactic signalling controls lysosomal function

To identify genes and pathways affected by chemoattractant-induced chemotaxis, we used a zebrafish *cxcr3.2* null model which displays attenuated macrophage motility and aberrant macrophage recruitment to infection foci (**Figure 1**)[10]. By deep-sequencing analysis of FACS-sorted *cxcr3.2* mutant and wildtype (wt) *mpeg1:mCherry-F*-positive macrophages, we found 699 significantly regulated genes. Using gene enrichment analysis tools we classified the regulated genes according to the affected pathways, cellular components, molecular functions and biological processes (**Table 1-2**). These functional analyses suggested alterations in lysosome biogenesis/maturation, Golgi-to-lysosome vesicular trafficking and lysosomal maintenance. Classification of gene products according to their cellular localisation also revealed that lysosome- and Golgi-related genes are mostly upregulated in the *cxcr3.2* mutants (**Figure 2**). Taken together, these data suggest that a coordinated induction of lysosomal genes takes place in *cxcr3.2* mutant macrophages and that Cxcr3.2 signalling exerts a negative transcriptional control on lysosomal biogenesis and function.

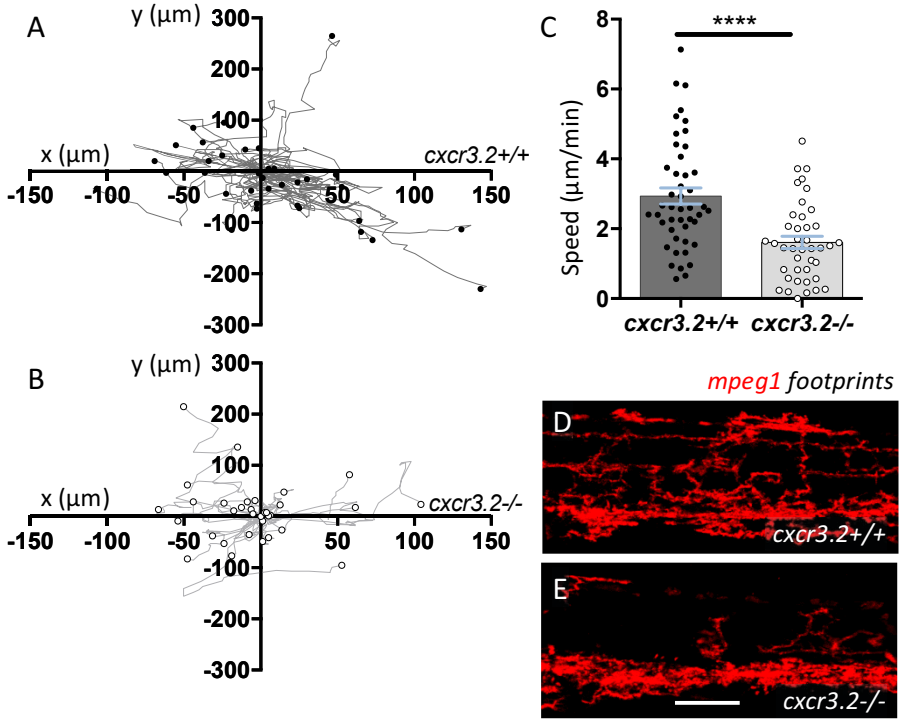

Figure 1. *cxcr3.2* mutation affects macrophage basal motility. A-B. XY plot of *cxcr3.2*$^{+/+}$ and *cxcr3.2*$^{-/-}$ macrophage tracks; **C.** Average speed of wt and mutant macrophage movement; **D-E.** Representative macrophage footprints in a wt and a mutant embryo during the time of observation Mutant and wt siblings expressing *Tg(mpeg1:mCherry-F)* were imaged at 2 dpf in the trunk area (1 h track, 1 frame/2 min, 63x objective). Scale bar: 100 µm. Data derive from 2 cumulated experiments, run with 3 mutants and 3 wt each.

KEGG-pathways				
Term	**Count**	**P-Value**	**Fisher Exact**	**Fold Enrichment**
Endocytosis	17	4,5E-03	1,9E-03	2,2
Lysosome	13	3,6E-03	1,3E-03	2,6
Neurotrophin signalling pathway	13	5,8E-03	2,1E-03	2,5
Tight junction	12	2,6E-02	1,1E-02	2,1
PPAR signalling pathway	12	1,3E-04	2,6E-05	4,1
Leukocyte transendothelial migration	12	1,1E-02	4,0E-03	2,4
Antigen processing and presentation	10	7,9E-03	2,5E-03	2,8
Adipocytokine signalling pathway	10	1,8E-03	4,6E-04	3,5
GO:Cellular components				
Term	**Count**	**P-Value**	**Fisher Exact**	**Fold Enrichment**
Cell				
Perinuclear region of cytoplasm	24	4,00E-04	1,60E-04	2,3
Vacuole	20	2,40E-03	1,00E-03	2,2
Lysosome	17	4,90E-03	2,00E-03	2,2
Pigment granule	13	9,40E-05	2,10E-05	4
Coated vesicle	12	3,20E-02	1,40E-02	2,1
Membrane				
Basolateral plasma membrane	17	3,30E-03	1,40E-03	2,3
Membrane raft	12	1,60E-02	6,50E-03	2,3
Organelle outer membrane	13	4,20E-04	1,10E-04	3,4
Cytoplasmic vesicle membrane	12	1,30E-02	5,20E-03	2,3
GO:Molecular functions				
Term	**Count**	**P-Value**	**Fisher Exact**	**Fold Enrichment**
Transporter activity				
Inorganic cation TMT activity	15	1,6E-03	5,6E-04	2,6
Monovalent inorganic TMT activity	12	1,8E-03	5,2E-04	3,1
Hydrogen ion TMT activity	10	6,5E-03	2,0E-03	3
Anion TMT activity	13	9,3E-03	3,6E-03	2,4
Primary active TMT activity	10	4,0E-02	1,7E-02	2,2
P-P-bond-hydrolysis-driven TMT activity	10	4,0E-02	1,7E-02	2,2
Protein binding				
Protein complex binding	16	7,0E-03	3,0E-03	2,2
Unfolded protein binding	15	1,0E-04	2,6E-05	3,5
Heat shock protein binding	10	1,7E-03	4,3E-04	3,6
Transcription corepressor activity	12	2,1E-02	8,5E-03	2,2
Cysteine-type peptidase activity	11	4,0E-02	1,7E-02	2,1

Table 1. KEGG-pathways, cellular components and molecular functions affected in *cxcr3.2* mutants. Terms related to lysosomes are marked in grey. See Materials and Methods for more details. TMT: transmembrane transporter.

GO:Biological processes				
Term	**Count**	**P-Value**	**Fisher Exact**	**Fold Enrichment**
Biological regulation				
Regulation of cell death	66	5,0E-09	2,2E-09	2,2
Response to organic substance	61	4,3E-09	1,8E-09	2,3
Negative regulation of molecular function	28	1,5E-04	6,2E-05	2,2
Small GTPase mediated signal transduction	25	5,1E-04	2,2E-04	2,2
Negative regulation of catalytic activity	23	7,6E-04	3,2E-04	2,2
Regulation of binding	18	6,0E-05	1,7E-05	3,1
Response to bacterium	18	9,6E-04	3,5E-04	2,5
Regulation of cell motion	16	6,1E-03	2,5E-03	2,2
Regulation of transcription factor activity	14	1,2E-04	3,0E-05	3,6
Regulation of I-kappaB kinase/NF-kappaB cascade	13	6,6E-04	1,8E-04	3,2
Response to oxidative stress	13	2,1E-02	8,9E-03	2,1
Negative regulation of protein modification process	12	5,1E-03	1,7E-03	2,7
Regulation of immune effector process	11	4,5E-03	1,4E-03	2,9
Negative regulation of response to stimulus	11	4,2E-03	1,3E-03	2,9
Innate immune response	11	3,5E-02	1,5E-02	2,1
Detection of stimulus	10	3,3E-02	1,3E-02	2,3
Cellular process				
Cell death	56	3,4E-07	1,5E-07	2,1
Membrane organisation	32	4,3E-05	1,8E-05	2,2
Mitochondrion organisation	14	2,0E-03	6,8E-04	2,7
Histone modification	10	4,0E-02	1,7E-02	2,2
Protein folding	19	1,2E-04	3,7E-05	2,9
Regulation of translation	11	3,3E-02	1,4E-02	2,1
Localisation				
Intracellular transport	51	1,4E-06	6,4E-07	2,1
Protein targeting	17	7,1E-03	3,1E-03	2,1
Golgi vesicle transport	14	1,3E-03	4,0E-04	2,8
Nucleocytoplasmic transport	14	5,8E-03	2,2E-03	2,4
Organic acid transport	12	2,3E-02	9,9E-03	2,2
Protein localisation in organelle	13	8,8E-03	3,4E-03	2,4
Protein import	12	1,0E-02	3,8E-03	2,4
Metabolic process				
Monosaccharide metabolic process	18	4,2E-03	1,8E-03	2,2
Carbohydrate catabolic process	14	2,2E-04	5,6E-05	3,4
Purine ribonucleotide metabolic process	11	3,5E-02	1,5E-02	2,1

Table 2. Biological processes affected in *cxcr3.2* mutants. Terms related to lysosomes are marked in grey. See Materials and Methods for more details.

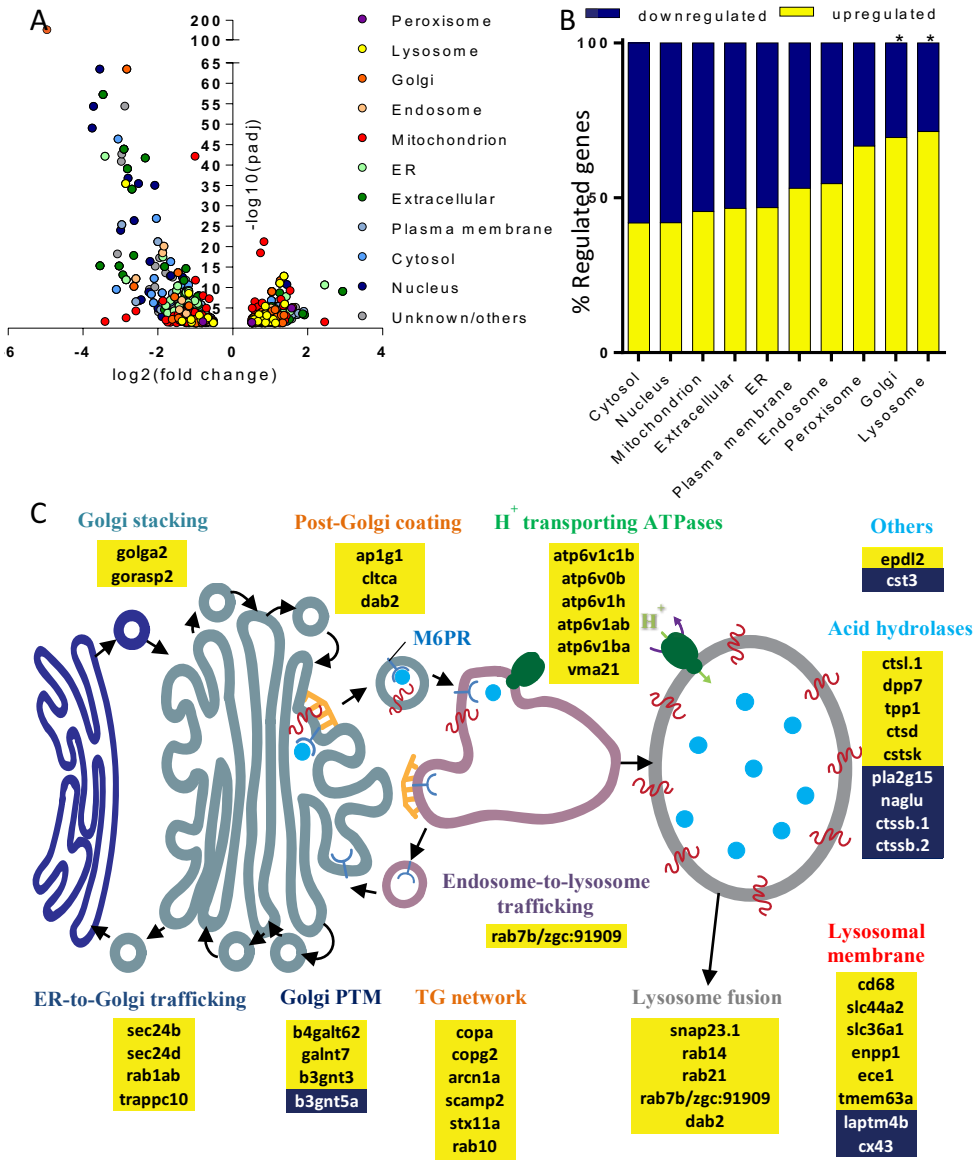

Figure 2. Graphical representation of enrichment analysis. **A.** Volcano plot representing the dispersion of the regulated genes. To note, while *cxcr3.2* mutation generally seems to affect target genes by downregulation (negative log2(fold change)), lysosomal genes are mostly affected towards upregulation (yellow). **B.** % upregulated (yellow) and downregulated (blue) genes classified by compartment. Chi-squared test analysis (with Bonferroni *post-hoc* correction for False Discovery Rate) shows that lysosome- and Golgi-related genes are significantly coordinated towards upregulation and diverge from the general trend of the other regulated genes. To note, not necessarily genes were univocally assigned to one single compartment. **C.** Functional classification of key Golgi- and lysosome-related genes affected by *cxcr3.2* deficiency. Gene names in yellow boxes indicate upregulated genes, while gene names in blue boxes indicate downregulated genes. ER: Endoplasmic reticulum; PTM: post translational modification; TG: trans-Golgi; M6PR: mannose-6-phosphate receptor.

Deficiency in *cxcr3.2* signalling affects intra-macrophage replication of mycobacteria

To quantify the lysosomal content of *cxcr3.2*$^{-/-}$ and *cxcr3.2*$^{+/+}$ macrophages, we stained lysosomes using LysoTracker, which is permeable in zebrafish larvae by bath exposure[16]. Notably, macrophages in *cxcr3.2* mutant embryos displayed an increased staining when compared to wt (**Figure 3A**). To determine whether the lysosomal function is dysregulated in *cxcr3.2* mutant macrophages, we injected pH-rodo labelled *E. coli* bioparticles and quantified phagosome acidification *in vivo*. In *cxcr3.2*-deficient embryos, the level of acidification at 30-45 minutes post injection (mpi) was significantly increased (~2 fold), indicating that lysosomes are still functional and that phagolysosome maturation is increased by *cxcr3.2* deficiency (**Figure 3B-D**). Therefore, both RNA-sequencing analysis and functional *in vivo* assays suggested an increased lysosomal function.

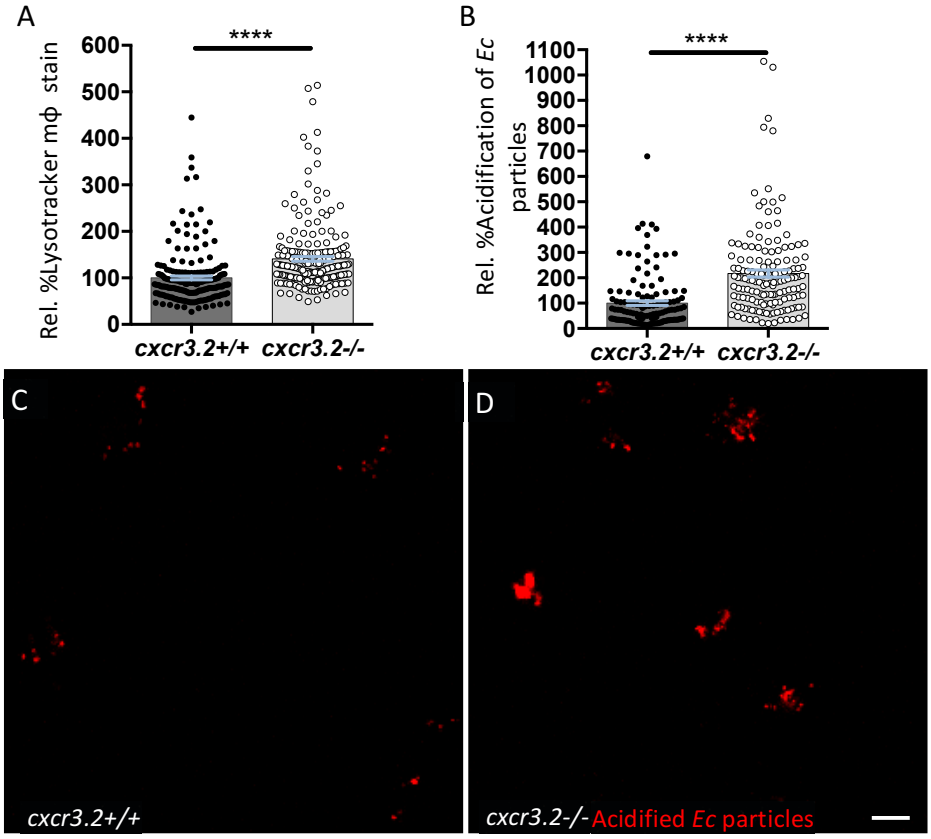

Figure 3. cxcr3.2 mutant macrophages display augmented lysosomal function and phagolysosome maturation. A. % (relative to wt) of LysoTracker intensity staining overlapping with the macrophage (mΦ)-specific *mpeg1:mCherry-F* transgene in 2 dpf mutant and wt siblings. Data derive from >12 individuals per group. Each data point represents a single *mpeg1:mCherry-F* cluster. 1 representative of 2 similar replicates. **B.** % (relative to wt) of pH-rodo intensity of *E. coli* bioparticle clusters at 30-45 mpi. Mean intensity was calculated per *E. coli* bioparticle cluster. Data derive from 12 individuals per group injected in experimental groups of 3-4 mutants and 3-4 wt. 1 representative of 2 similar replicates. **C-D.** Representative images of the yolk valley of a wt and mutant embryo at 30 minutes post *E. coli* bioparticle injection (63x objective). Scale bar: 10 μm.

To evaluate whether the enhanced lysosomal functionality results in better infection control, we investigated the capability of *cxcr3.2* mutant macrophages to counteract initial infection with the intra-macrophage bacterial parasite *M. marinum* strain M (*Mm*M), a wt isolate of the natural fish pathogen, which represents an established paradigm to study human mycobacterial diseases, such as tuberculosis and leprosy[17,18,19,20]. As expected, the acidification of *Mm*M (24-28 hours post infection, hpi) was increased in *cxcr3.2* mutants (**Figure 4A**). To assess the basal intracellular killing ability of macrophages in wt and *cxcr3.2* mutant embryos, we injected *MmΔerp* bacteria[21,22,23] and scored the capability of macrophage to contain the infection at 44 hpi. Consistent with previous acidification results, we found the intracellular killing of *MmΔerp* to be significantly increased in *cxcr3.2* mutants (**Figure 4B-C**).

We have previously shown that *cxcr3.2* mutants display deficient macrophage-dependent mycobacterial dissemination and a reduced expansion rate of granuloma-like structures, which was attributed to the reduced macrophage trafficking within the granulomatous lesions[10]. However, the assays used here are performed at an initial infection stage that precedes the granulomatous phase. Furthermore, *MmΔerp* stain fails to induce macrophage aggregation[21]. Additionally, since bacteria are systemically delivered, the direct implication of macrophage recruitment at this stage is unlikely, as all bacteria are readily available to circulating macrophages and are rapidly phagocytosed. Of note, the level of intracellular bacteria at 30 mpi (*Mm*M) and the number of established intra-macrophage infectious niches at 44 hpi (*MmΔerp*) were found similar in *cxcr3.2* mutants and wt (**Figure 4D-E**), suggesting no difference in the level of initial phagocytosis and mycobacteria multiplicity per macrophage but only in their intramacrophage replication/killing rate. Taken together, these data show that *cxcr3.2* mutation, by increasing the lysosomal functionality, exerts a bacteriostatic function and antagonises intra-macrophage bacterial replication.

Cxcr3.2 controls macrophage polarity and lysosome localisation to the leading edge

Previous *in vitro* studies linked CXCR3 signalling to lysosomal function. Stimulation of chemokine-dependent motility affected localisation of lysosomes into the cell and mediated their calcium-dependent fusion to the plasma membrane, a mechanism also known as lysosome exocytosis[5]. Despite that LysoTracker staining could not be trusted to quantify the occurrence of exocytosis in terms of signal decrease during cell migration (due to high frequency of image acquisition and high laser intensity, provoking bleaching) we could use this vital staining to determine whether macrophages displayed asymmetrical lysosome distribution during cell migration *in vivo*. Strikingly, we could establish that in wt macrophages, lysosomes are significantly localised to the leading edge of the moving cell, while their position remained central or non-correlated in non-moving macrophages (**Figure 5**, **Supplementary Movie 1-2**). In contrast, in *cxcr3.2*-deficient embryos, the lysosomal content of macrophages did not correlate with the movement of the cell. These observations strongly suggest that a *cxcr3.2*-dependent signalling is required to maintain lysosomal recruitment to the leading edge and anterior-posterior macrophage asymmetry.

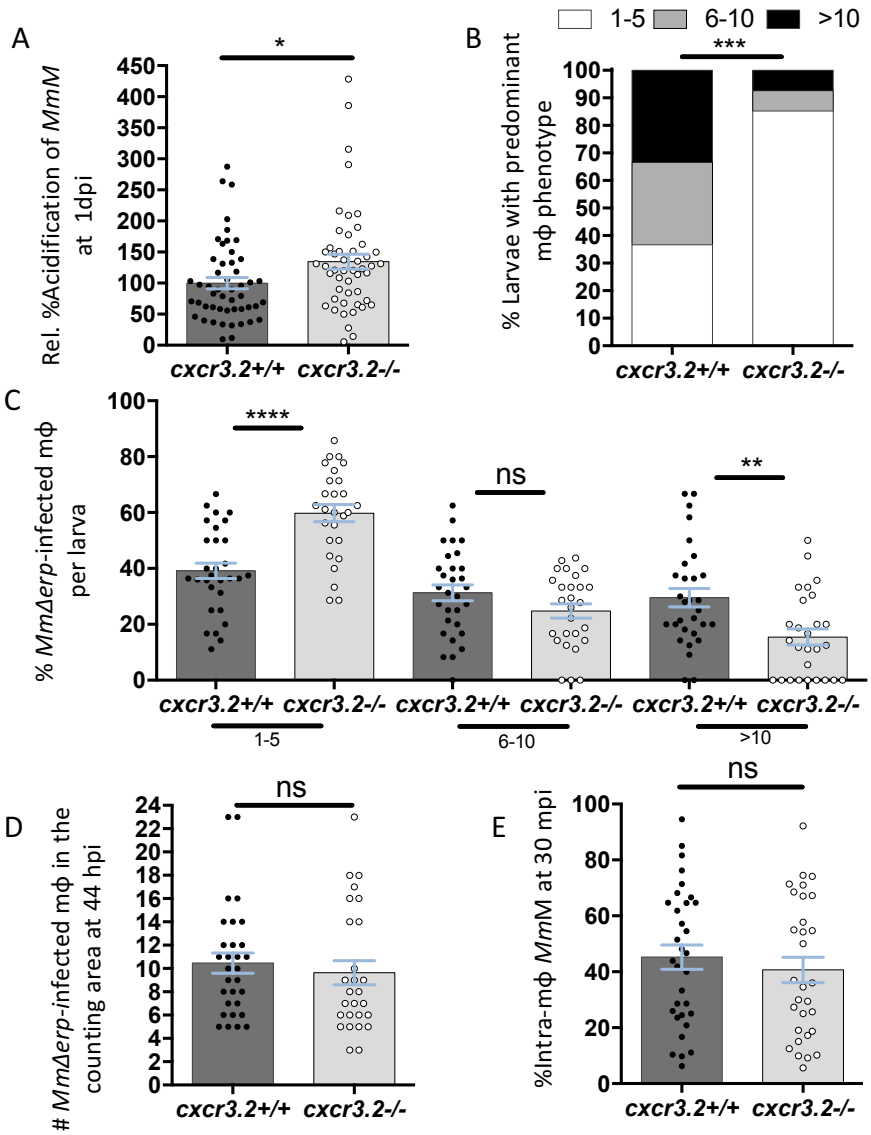

Figure 4. *cxcr3.2* mutant macrophages counteract more efficiently initial mycobacterial replication. A. % (relative to wt) of LysoTracker intensity staining of *Mm*M in mutant and wt at 1dpi. Data derive from >22 mutant or wt embryos per group per replicate. Each data point represents a single embryo. The graph is cumulative of 2 experiments. **B-D.** Intracellular replication of *MmΔerp.* At 44 hpi intra-macrophage sites of bacterial growth were classified into three categories according to the number of bacteria (1-5, 6-10 or >10). In B, larvae were classified according to the predominant macrophage phenotype. C represents the % of macrophages per larva in each class. D represents the number of intra-macrophage *MmΔerp* sites at 44hpi. B-D are cumulative of 2 experiments performed each with >10 individuals per group. **E.** Phagocytosis of *Mm*M at 30 mpi in mutant and wt.

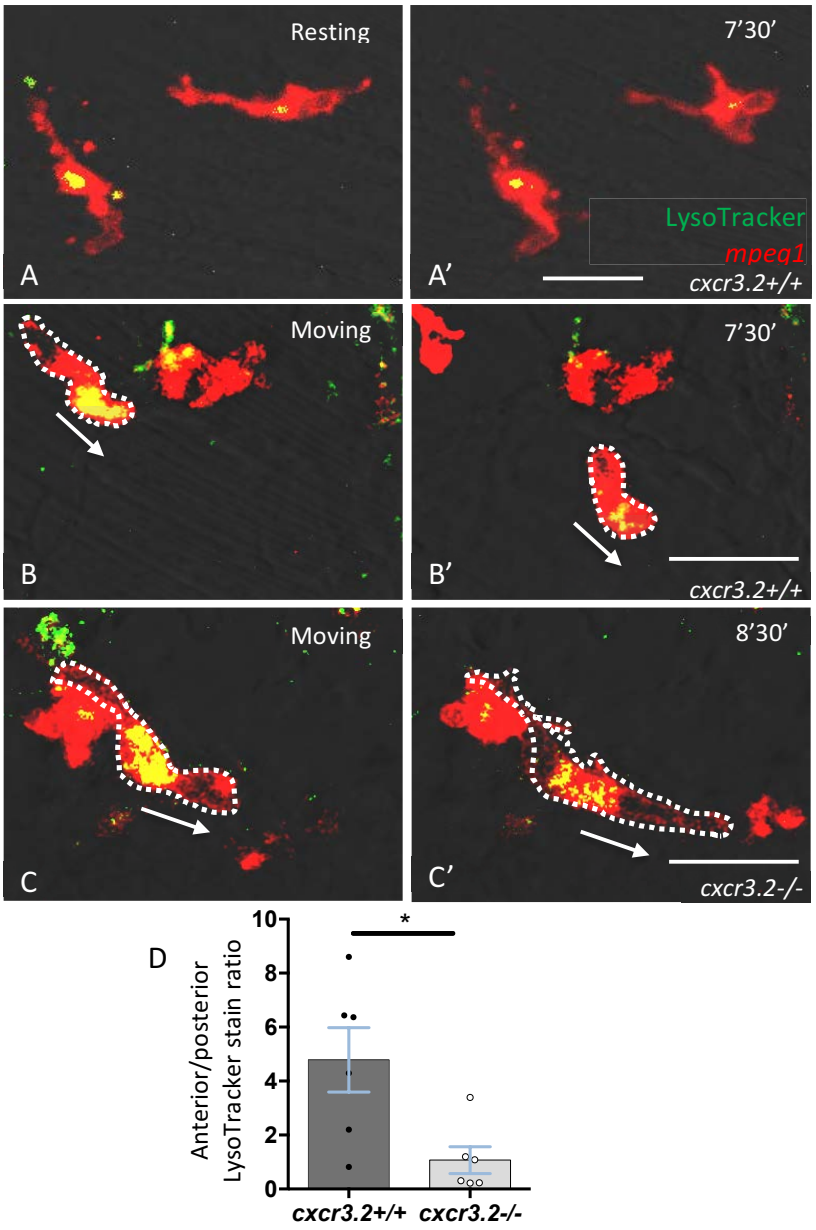

Figure 5. *cxcr3.2* controls localisation of lysosomes to the leading edge of moving macrophages. **A-A'.** Immotile wt macrophages with central LysoTracker staining. **B-B'.** Moving wt macrophage with LysoTracker staining highly committed to the lamellipodium. **C-C'.** Moving mutant macrophage with LysoTracker staining not associated with the leading edge. **D.** Ratio of LysoTracker staining between the anterior and posterior half of moving macrophages in wt and mutant Each data point indicates a single tracked cell from an independent embryo (N: 6 cells/group). Images were acquired at 2 dpf (40x objective rate < 1 photogram/30 sec) and the time interval between images from the same cell is indicated. See also **Supplementary Movie 1-2**. Scale bars: 20 µm.

Infected macrophages express Cxcl11aa via Myd88-dependent immune recognition

We previously demonstrated that *cxcl11aa* is highly upregulated during mycobacterial infection[10]. To determine the source of Cxcl11aa, we FACS-sorted *mpeg1:mCherry-F* positive macrophages from *Mm* infected and mock-injected larvae and quantified the level of *cxcl11aa* expression in the fluorescent (macrophages) and unlabelled (negative) cell fraction. In uninfected conditions, the expression of *cxcl11aa* was significantly enriched in the macrophage cell fraction (**Figure 6A**). This finding is in agreement with the function of Cxcr3.2 in the maintenance of the basal macrophage patrolling, which is most likely exerted via a chemokinetic autocrine/paracrine mechanism[10]. Additionally, during infection, macrophages significantly upregulated the expression levels of *cxcl11aa* (**Figure 6A**).

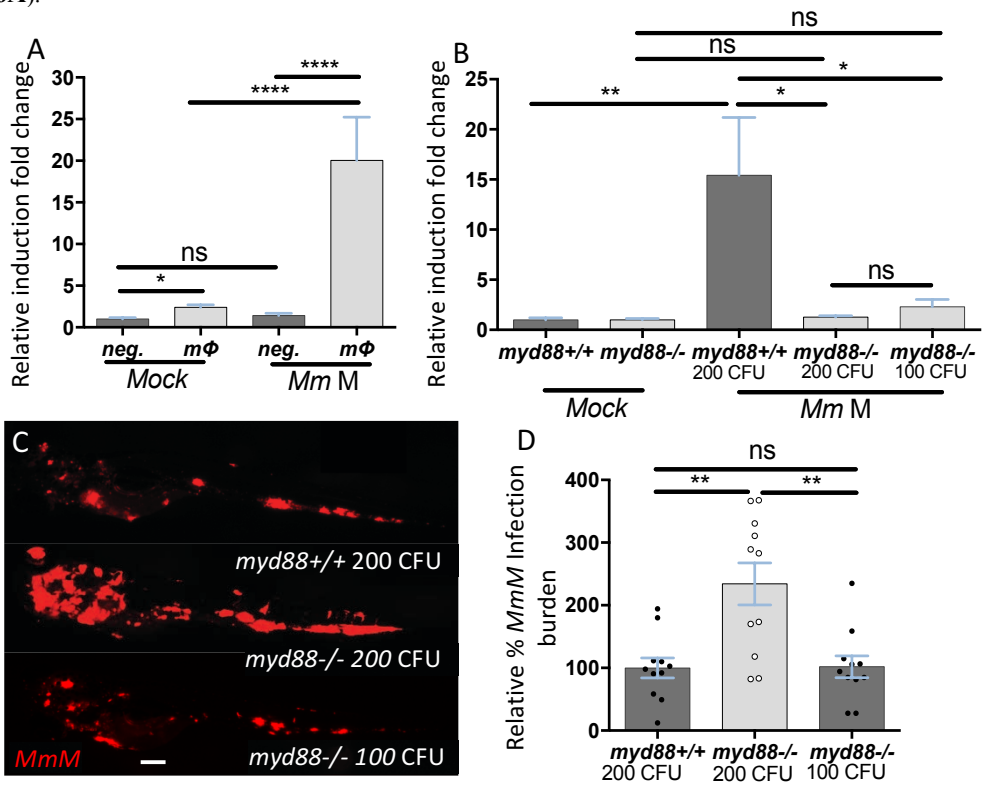

Figure 6. *cxcl11aa* expression is upregulated in macrophages upon infection and requires an active Myd88-immune signalling. A. Expression of *cxcl11aa* in *Tg(mpeg1:mCherry-F)* sorted cells and its infection-dependent induction (relative to negative/mock fraction). *Mm*M- (or mock-) injected larvae (>100 per replicate per condition) were dissociated at 5 dpi. Results are cumulative of two independent experiments each run by collecting 4 samples per condition. **B-D.** Dependency of *cxcl11aa* induction from *myd88*. qRT-PCR samples (B), representative burden pictures (C) and representative burden analysis (D) derive from larvae collected at 4 dpi. Results in B (folds relative to mock) are cumulative of two independent experiments each run by collecting 3 samples (pools of >10 individuals) per condition. Each point in D represents 1 infected larva from a representative pool. Scale bar: 200 µm.

Notably, this did not require the bacterial locus RD1 (Region of Difference 1), a pathogenicity locus encompassing the secretion system of ESAT-6 (Early Secreted Antigenic Target 6 kDa), which is associated with mycobacterial virulence and formation of tubercular granulomas[24] (**Supplementary Figure 1**).

Next, we asked whether *cxcl11aa* induction requires the central immune mediator Myd88, which links pathogen recognition by Toll-like receptors to activation of the transcription factor Nfκb[25]. Therefore, we quantified the expression levels of Cxcl11aa in *myd88* deficient larvae. Since *myd88* mutants display an increased infection level when infected with the same initial infection load as wt siblings[25], we compensated this with a reduced inoculum, to obtain a similar infection level at 4 days post infection (**Figure 6B-D**). Both with the reduced and the regular inoculums, *myd88* mutants displayed a marked incapability to upregulate *cxcl11aa*, indicating that transduction of an active Myd88/Nfκb signalling is key to upregulate macrophage production of Cxcl11aa (**Figure 6B)**. In agreement with this, we observed that Nfκb activation is also required to maintain the random patrolling of macrophages under uninfected conditions, suggesting that Myd88/Nfkb signalling is required for both induction and constitutive expression of *cxcl11aa* (**Supplementary Figure 2**).

Based on our results, we propose a novel mechanism by which mycobacteria recognition can trigger acquisition of a permissive (lysosome-low) macrophage phenotype. Intracellular infection leads to immune recognition via Myd88. This, in turn, leads to induction of *cxcl1aa* and autocrine activation of its cognate chemokine receptor Cxcr3.2. Since in the absence of the Cxcr3.2-mediated pathway transcription of lysosomal genes is enhanced, wt activation of Cxcr3.2 signalling might contribute to attenuate the lysosome function and facilitate their exocytosis by controlling their recruitment to the leading edge. These effects would dissipate the innate capability of macrophages to counteract infection via lysosomal acidification and, therefore, increase the chances of successful establishment of an intracellular replication niche.

DISCUSSION

Lysosomes have long been known as cellular organelles that are principally involved in degradation and recycling of senescent/damaged cellular parts and undesired cytosolic contents, such as unfolded proteins and invading microbes. However, much broader functions for lysosomes are recently emerging. Not only have lysosomes been shown to function as signalling centres that control cellular adaptation to environmental cues, but lysosomes have also been shown to play a critical role in cell migration. Here we report a novel link between chemotactic signalling and transcriptional regulation of lysosomal function. Our study of a zebrafish mutant in the orthologue of chemokine receptor CXCR3 demonstrates that upregulation of lysosomal gene expression due to suppressed CXCR3-dependent motility can prime macrophages to better control intracellular infection. Furthermore, we show that mycobacterial parasitism activates this chemokine signalling cell-autonomously in the host macrophages, which suggests that intracellular mycobacterial colonisation, by exploiting CXCL11-CXCR3 signalling, might attenuate the lysosomal function and facilitate the establishment of parasitosis.

CXCR3 is best known for its expression by T cells, but evidence that this receptor is crucial to control the function of monocyte/macrophage lineages (including tissue

macrophages[8,9], perivascular macrophages[12], tumour associated macrophages[13], microglial[14], Kupffer[15] and dendritic cells[26,27]) continue to emerge, with a range of implications spanning from chemotaxis to cell homoeostatic maintenance and regulation of gene expression. Notably, expression of CXCR3 orthologues by the myelomonocytic lineages (and its chemotactic properties towards CXCL9-10-11 cues) is conserved among vertebrates, from fish to mammals[6,7,8,9,10,12,28,29,30]. We previously described that macrophage motility and recruitment to infectious foci is attenuated in zebrafish carrying a null mutation in *cxcr3.2*, the orthologue of mammalian *CXCR3*. Furthermore, we found this mutation to be associated with increased resistance to tuberculosis caused by *Mm* infection. Here, by analysing the transcriptional signature dependent on Cxcr3.2*,* we found that the presence of this receptor on macrophages affects the transcriptional control of lysosomal genes. Failure to execute the Cxcr3.2-dependent pathway in null mutants led to a transcriptional reprogramming of macrophages, characterised by a predominant upregulation of genes involved in Golgi and lysosomal vesicle trafficking as well as various lysosomal genes, including proton-transporting ATPases and endopeptidases, for example cathepsin L. By functional *in vivo* assays we subsequently demonstrated that mutation of *cxcr3.2* also prevents lysosome polarisation during macrophage migration, and, as a consequence of the upregulation of lysosomal genes, *cxcr3.2*-deficient macrophages display an increased lysosomal content, an increased acidification rate of bacteria-containing compartments and enhanced *Mm* killing.

The link between lysosomal function and chemotaxis has only recently emerged. Chemotactic signals, by stimulating an increase in cytosolic calcium, enable migration of lysosomes to the leading edge of moving cells[5]. At the leading edge, high levels of cytosolic calcium mediate formation of SNARE complexes by modulating the activity of proteins of the synaptotagmin family, including SYT7 and SYTL5. Synaptotagmins, together with specific RABs, permit docking and fusion of lysosomes to the plasma membrane (lysosomal exocytosis). This process is thought to facilitate cell migration by providing a source of phospholipid bilayer and by promoting the release of the uropod (trailing edge). Lysosome exocytosis has also been reported to occur for plasma membrane repair and for various secretion processes, for example by cytotoxic T-cells and mast cells[31,32]. Notably, apart from chemotactic triggers, lysosomal exocytosis has been described during several intracellular infections, including of mycobacterial nature[33].

In agreement with the *in vitro* evidence for the role of lysosomes in sustaining chemotaxis, our *in vivo* results demonstrate that Cxcr3.2-dependent signalling controls localisation of lysosomes in the moving cell at the leading edge, the site where they eventually exocytose. Our study additionally revealed that reduced transduction of chemokine signals can affect lysosomal maintenance also at transcriptional level, since depletion of *cxcr3.2* led to upregulation of lysosomal gene expression. The existence of a concerted transcriptional basis that controls lysosomal homoeostasis is consistent with recent reports[34]. The master transcription factor EB (TFEB) was reported to control the Coordinated Lysosomal Expression and Regulation (CLEAR) gene network[35]. Under aberrant lysosomal storage conditions, or when lysosomes are under stress (for example during the response to infections), TFEB dissociates from the lysosome surface and translocates to the nucleus where it promotes direct transcription of lysosomal genes. We suspect that reduced trafficking of lysosomes, as a consequence of abolished basal motility in *cxcr3.2* mutants, may be sensed as a stressor and lead to activation of the CLEAR response, which in turn will increase intracellular lysosome content and thereby prime Cxcr3.2-deficient

macrophages to better withstand infection. In line with this hypothesis, it has been reported that TFEB and the CLEAR-network are activated to increase the pool of lysosomes in the proximity of the plasma membrane and to promote their exocytosis[36]. Interestingly, this mechanism is mediated by raising intracellular Ca^{2+} levels through the activation of lysosomal Ca^{2+} channels, differently from chemokine-based Ca^{2+} fluxes, which mostly derive from IP3-dependendent modulation of endoplasmic reticulum storage. This may suggest that the CLEAR response in the chemotactic-deficient conditions of *cxcr3.2* mutants attempts to restore normal lysosome trafficking by stimulating the alternative mobilisation of Ca^{2+} from lysosomal storage. Notably, the CLEAR network appears to be involved in the regulation of additional lysosome-associated processes, including autophagy, exo/endocytosis, melanogenesis, phagocytosis, and immune response, as well as in several non-lysosomal responses, such as expression of digestive enzymes, genes related to sugar metabolism, MAPK signalling, adipocytokine signalling pathway, chemokine signalling etc[37]. This might in part explain why several of these CLEAR-related pathways appear regulated also in our study (**Table 1-2**).

Multiple genetic diseases, including lysosomal storage disorders such as Gaucher's, Niemann-Pick's disease and Tay-Sachs syndrome, are associated with impaired lysosomal function and increased susceptibility to infections[38,39,40]. Knockdown of the zebrafish orthologues of three genes linked to lysosomal storage disorders in man (*glucocerebrosidase 1*, *hexosaminidase A*, and *arylsulfatase A*) was recently found to result in hypersusceptibility to tuberculosis[41]. Similarly, knockdown of the gene for cathepsin L and mutation of a transcriptional coregulator, Snapc1b, which regulates cathepsin L, caused tuberculosis hypersusceptibility in the zebrafish model[41]. All these genetic deficiencies are associated with an inability of macrophages to contain the mycobacterial infection due to a severe migration defect that results from the progressive accumulation of cellular debris in lysosomes[41]. A comparable defect is found in zebrafish mutants in components of Rag-regulator complex, which is part of the CLEAR network[42]. In these mutants, microglial cells (the resident macrophages of the brain) are unable to digest apoptotic neurons despite an expanded lysosomal compartment. Adding to these studies, our work reveals that lysosome function can be genetically enhanced by a transcriptional response that is directly linked with chemotactic signalling. Macrophages in *cxcr3.2* mutants are still able to migrate normally in response to Cxcr3.2-independent cues, but their basal motility and ability to disseminate mycobacterial infection are reduced[10]. We propose that these altered chemotactic responses together with the enhanced lysosomal function act synergistically to increase the resistance of *cxcr3.2* mutants to tuberculosis. In addition, we have shown that, by exploiting a Myd88-dependent signalling axis, mycobacteria can increase the expression of Cxcl11aa, the cognate ligand of Cxcr3.2. This implicates that immune recognition of the pathogen can lead to activation of the chemokine/lysosome circuit that will ultimately suppress the antimicrobial capability of the host cells.

The regulative function exerted by CXCR3 on lysosomal maintenance seems to be conserved between zebrafish and mammals. A previous study in CXCR3-knockout mice revealed that microglial cells can eliminate more efficiently amyloid deposits and prevent the onset of Alzheimer disease more efficiently in CXCR3-deficient conditions. This phenotype was, at least partly, due to an increased size of the lysosomal compartment and to a more efficient maturation of phagolysosomes occurring in these cells[14]. Furthermore, CXCR3 expression was linked to diet-induced steatohepatitis (liver inflammation with fat

accumulation) through induction of lipogenic genes and impairment of autophagolysosome maturation. In this model, pharmacological blockade of CXCR3 using receptor antagonists could reverse the disease and facilitated clearance of lipid inclusions[15].

Taken together, our work indicates that CXCR3-CXCL11 signalling exerts multiple functions on macrophages during the inflammatory processes, by controlling their initial recruitment to infection foci, their reverse migration facilitating tissue dissemination of mycobacteria, their motility during granuloma formation and, as shown in here, their intrinsic microbicidal/degradative capabilities. Mycobacteria seem to have evolved multiple mechanisms for manipulating this signalling axis to regulate macrophage trafficking to the infection focus, drive macrophage-dependent dissemination and ultimately suppress the basal bactericidal property of the host cell. Application of anti CXCR3-therapies may, therefore, represent a valuable strategy to combat mycobacterial diseases on multiple fronts, and possibly to counteract also other non-infectious diseases that arise from lysosomal dysfunctions.

MATERIALS AND METHODS

Zebrafish lines and maintenance – Zebrafish lines were handled in compliance with the local animal welfare regulations and maintained according to standard protocols (zfin.org). The breeding of fish lines was approved by the local animal welfare committee (DEC) of Leiden University (license number: 10612) and adhered to the international guidelines specified by the EU Animal Protection Directive 2010/63/EU. All experiments were performed on embryos/larvae that had not reached the stage of independent feeding. Fish lines used in this work were the following: the macrophage reporter line *Tg(mpeg1:mCherry-F^{ump2})*[43], *(cxcr3.2^{hu6044})*[10] homozygote mutant (*cxcr3.2$^{-/-}$*) and wildtype (*cxcr3.2$^{+/+}$*) siblings, the combination of (*cxcr3.2^{hu6044}*) allele with *Tg(mpeg1:mCherry-F^{ump2})*, and the (*myd88^{hu3568}*)[25] homozygote mutant (*myd88$^{-/-}$*) and wildtype (*myd88$^{+/+}$*) siblings. Embryos were generally maintained at 28.5°C in egg water (60 µg/ml sea salt, Sera Marin, Heinsberg, Germany). For pH sensitive experiments (pH-rodo acidification assay, LysoTracker staining), embryos were placed in E2 medium (15 mM NaCl; 0.5 mM KCl, 1.0 mM MgSO4, 150 µM KH_2PO_4, 50 µM Na_2HPO_4, 1mM $CaCl_2$; 0.7 mM $NaHCO_3$) at least 6 h before the experiment and maintained in E2 medium during the experimental work. Larvae destined to image acquisition were maintained in medium water supplemented with 0.003% PTU (1-phenyl-2-thiourea; Sigma-Aldrich, St Louis, MO, USA) from ~8 hpf to prevent pigmentation. Anaesthesia of embryos/larvae was achieved with 0.02% buffered Tricaine (3-aminobenzoic acid ethyl ester; Sigma-Aldrich) in egg water or E2 medium.

FACS-sorting, RNA isolation, cDNA preparation and RNA-sequencing analysis – *mpeg1:mCherry-F*-positive and unlabelled cells were sorted from *Tg(mpeg1:mCherry-F/cxcr3.2$^{-/-}$)* and wt siblings at 6 dpf. Dissociation of larvae and FACS was performed according to reference[44]. RNA was obtained using the miRNeasy mini kit (Qiagen), and residual genomic DNA was eliminated by DNase treatment (RNase-Free DNase Set, Qiagen). cDNA preparation was performed using the SMARTer® Universal Low Input RNA Kit for Sequencing (Clontech) according to the manufacturer's guidelines. Illumina RNA sequencing and the mapping and counting of reads was outsourced to ZF-screens (Leiden, the Netherlands) and performed as in reference[44]. Statistical analysis of the read count data was performed using the DESeq2 bioinformatic package

(https://bioconductor.org/packages/release/bioc/html/DESeq2.html)[45] and default settings for paired analysis test, using triplicate data sets of *mpeg1:mCherry-F* positive cells, derived from three pools of > 150 larvae/each, obtained from three independent group crosses of *cxcr3.2*$^{-/-}$ and *cxcr3.2*$^{+/+}$. Before processing, lowly expressed genes (sum of reads from three mutant and three wt replicates < 50 total reads), were removed. For gene ontology analysis, we selected significantly expressed genes using a p.adj < 0.05 and |log2(fold change)| > 0.5 cut off. Significantly affected KEGG-pathways, GO:cellular components, GO:molecular functions or GO:biological processes (**Table 1-2**) were predicted by submission of the list of human orthologues of the significantly regulated zebrafish genes to DAVID bioinformatic tools (https://david.ncifcrf.gov)[46]. Zebrafish-human orthologous correspondences were derived from g:profiler (http://biit.cs.ut.ee/gprofiler)[47] and curated with manual annotations (zebrafish gene products that did not have an annotated human orthologue were assigned to the closest human orthologue based on the same gene name or high protein sequence identity when blasted to the Ensembl human protein database; genes that did not have any clear human orthologue were discontinued). The cut-off for gene enrichment analysis was set to p.value < 0.05, Fisher Exact test < 0.05, number of affected genes ≥ 10, fold enrichment > 2. To generate **Figure 2A-C**, genes were annotated to compartments according to their GO:cellular component annotations (using Gene ontology annotation database available at geneontology.org). Genes could be associated with multiple compartments. Statistical divergence of Lysosome and Golgi-related genes from the general trend of the other regulated genes (**Figure 2 B**) was tested by chi-squared test analysis (with Bonferroni *post-hoc* correction for False Discovery Rate).

Microinjections, bacterial cultures and infection delivery – Where not differently specified, approximately 200 CFU of *Mycobacterium marinum* strain M (or where specified its isogenic mutant strains *Mm ΔerpA* or *Δrd1*) constitutively fluorescently labelled with eGFP, mCherry, mCrimson or Wasabi[22,48] were injected in a volume of 1-2 nl into the blood island/caudal vein of zebrafish embryos at 28-30 hpf. For the assessment of the microbicidal activity of macrophages against initial mycobacterial infection, a single-cell suspension of *MmΔerpA*-Wasabi was injected from -80°C frozen single-use aliquots, using a protocol adapted from reference[22]. Briefly, bacteria from a 1-week-old plate were inoculated to an OD600 of 0.2 in 10 ml 7H9 medium supplemented with ADC enrichment. The culture was grown for 24 h to reach an OD of 1.0. Bacteria were washed 3 times in Phosphate Buffer Saline (PBS) and suspended in PBS supplemented with 10% glycerol to an OD600 of 5.0. 50 µl aliquots were frozen in liquid nitrogen and stored at -80°C. Upon thawing, the vital bacteria were quantified by plating as being approximately 100 CFU/nl. In all the other cases, bacteria were prepared from a fresh culture as described in reference[10]. For the acidification assay (**Figure 3A-D**) 1 ng *E. coli* pH-rodo bioparticles conjugate for phagocytosis (Invitrogen) were injected into the blood island/caudal vein at 32-37 hpf and imaged over the yolk at 30-45 mpi. Similarly, for the phagocytosis assay (**Figure 4E**) *Mm*M-mCrimson bacteria were injected in *mpeg1:mCherry-F* individuals at 33-34 hpf, fixed at 30-32 mpi and imaged over the yolk as fixed samples (see below).

LysoTracker staining – For visualisation of acidic compartments, 2 dpf embryos were stained for 1-2 hours with 10 µM LysoTracker green DND-26 (Invitrogen) in E2 medium via bath exposure. Before imaging, embryos were quickly rinsed 3 times with E2 medium supplemented with Tricaine.

Imaging and image quantification – For still image and time-lapse acquisition, fixed or live embryos/larvae were mounted in 1.5-2% low-melting-point agarose (SphaeroQ, Burgos, Spain) and imaged with a Zeiss Observer 6.5.32 laser-scanning confocal microscope (Carl Zeiss, Sliedrecht, The Netherlands). To quantify LysoTracker acidification of macrophages (**Figure 3A**), the mean intensity of LysoTracker staining overlapping with the *mpeg1:mCherry-F* transgene at 2dpf was measured using Fiji/Image J quantification tools. Similarly, to quantify *Mm* acidification *in vivo* (**Figure 4A**) the mean intensity of LysoTracker staining overlapping with *Mm*M-mCrimson signal (1 dpi/2 dpf) was measured. To evaluate acidification of *E. coli* bioparticles (**Figure 3B**), the intensity of bioparticles clusters was analysed from pictures. % of phagocytosis of *Mm*M at 30 mpi was quantified as % of *Mm*M-Wasabi signal overlapping with *mpeg1:mCherry-F* signal (over the yolk) from fixed (O/N in 4% paraformaldehyde in Phosphate Buffer Saline supplemented with 0.08% of Triton X100) embryos. All images used for quantification in **Figure 3-4** were acquired with Plan-Neofluar 40x/0.9 Imm corr objective (Carl Zeiss). Data are expressed as % relative to wt (set to 100%). To score the microbicidal activity of macrophages against mycobacteria (**Figure 4B-C**), *Tg(mpeg1:mCherry-F)* embryos injected with Wasabi-labelled *MmΔerp* were fixed at 44 hpi, according to reference[23] and intra-macrophage mycobacterial sites of growth were counted (blind) using a C-Apochromat 63x/1.20 W Korr UV-VIR-IR objective (Carl Zeiss). In **Figure 4C**, the level of infection per macrophage was classified into three classes based on the severity of bacterial content (1-5 bacteria, 6-10 bacteria or >10 bacteria). In **Figure 4B**, each larva was assigned to one of these three classes according to its predominant macrophage phenotype (most frequently observed class of macrophage phenotype per individual larva). In case multiple classes showed the same percentage of macrophage phenotype, larvae were assigned to the most severe class among those.

Time-lapse analysis – The average speed and tracks of macrophages (**Figure 1, Supplementary Figure 2**) were calculated as previously described in reference[10], from movies acquired with an EC Plan-Neofluar 10x/0.30 M27 objective (Carl Zeiss) for 1 hour and an acquisition frequency of 2 minutes. Localisation of lysosomes to the leading edge (**Figure 5**, **Supplementary Movie 1-2**) was quantified by time-lapse imaging of LysoTracker-positive moving macrophages using Plan-Neofluar 40x/0.9 Imm corr objective and at an acquisition rate of <1 photogram/30 sec. The position of LysoTracker was quantified at the maximum extension of the cell during the time-lapse acquisition, by determining the ratio between the level of cell LysoTracker staining in the anterior and in the posterior half of the cell in the direction of movement.

qRT-PCR – To address dependency of *cxcl11aa* on *myd88* signalling, and the effect of bacterial infection on *cxcl11aa* induction, RNA was isolated from *myd88*$^{-/-}$ and *myd88*$^{+/+}$ whole larvae (infected with *Mm*M, **Figure 6B**) and from *cxcr3.2*$^{-/-}$ and *cxcr3.2*$^{+/+}$ larvae (infected with *Mm*M or its isogenic attenuated strain *MmΔrd1,* **Supplementary Figure 1**) at 4 dpi according to reference[10]. To address the macrophage specificity of *cxcl11aa* induction during infection (**Figure 6A**), we sorted the macrophage population of *Tg(mpeg1:mCherry-F)* line (and the unlabelled population) from infected or uninfected (mock injected) larvae at 5 dpi and extracted RNA as described above. cDNA synthesis, qRT-PCR protocol and analysis were performed as previously described in reference[10]. Expression of *cxcl11aa* was compared to *ppiab* for whole-mount analyses and to *eif5* for FACS sorted cells. Primers for these genes were: *cxcl11aaFw*: ACTCAACATGGTGAAGCCAGTGCT; *cxcl11aaRv*:

CTTCAGCGTGGCTATGACTTCCAT; *ppiabFw*: ACACTGAAACACGGAGGCAAAG; *ppiabRv*: CATCCACAACCTTCCCGAACAC; *eif5Fw:* CAAGTTTGTGCTGTGTCCCG; *eif5Rv:* AGCCTTGCAGGAGTTTCCAA.

Statistical analysis – Statistical significance was analysed using GraphPad Prism 6 (GraphPad Software, La Jolla, CA, USA). RNA sequencing statistical analysis was performed as described above in the dedicated section. Data in **Figure 1**, **Figure 3**, **Figure 4A** and **Figure 5** were statistically analysed by two-tailed *t*-tests. Individual two-tailed *t*-tests were used also to analyse the difference in % of macrophage phenotypic class upon infection (**Figure 4C**). Chi-squared contingency was used to test different distribution of larva phenotypes upon infection (**Figure 4B**). No difference in number of infected macrophages in the counting area (**Figure 4D**) was assessed by Mann-Whitney test. Differences in infection burden in **Figure 6D** and in cell speed in **Supplementary Figure 2** were statistically tested by Kruskal-Wallis test followed by Šidák comparison test of selected pairs. For qRT-PCR, statistical significance was estimated by two-tailed *t*-tests on ln(n)-transformed relative induction folds. Significance (*P*-value) is indicated with: ns, non-significant; *$P<0.05$; **$P<0.01$; ***$P<0.001$; ****$P<0.0001$. Error bars: mean±s.e.m.

ACKNOWLEDGEMENTS

We acknowledge Julien Rougeot and Tomasz Prasjnar for suggestions and discussions, especially related to the RNAseq data presentation and analysis. We also acknowledge Frida Sommer for valuable help and support.

This work was supported by the Smart Mix Program of the Netherlands Ministry of Economic Affairs and the Ministry of Education, Culture and Science, the European Commission 7th framework project ZF-HEALTH (contract number HEALTH-F4-2010-242048), and the European Marie-Curie Initial Training Network FishForPharma (contract number PITN-GA-2011-289209).

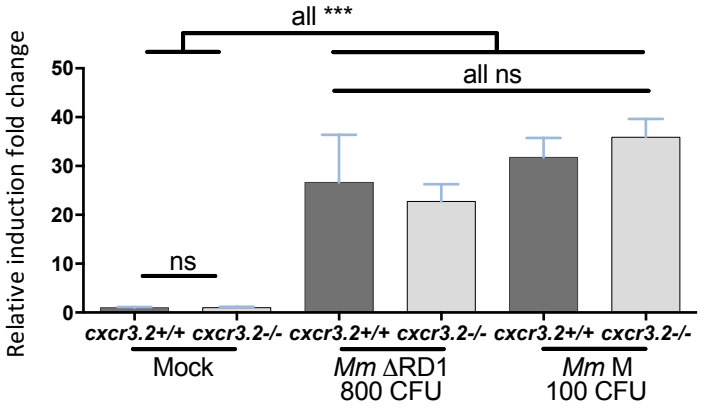

Supplementary Figure 1. cxcl11aa induction does not require the RD1 pathogenicity locus and *cxcr3.2* mutants are still able to upregulate *cxcl11aa* at comparable levels to wt.

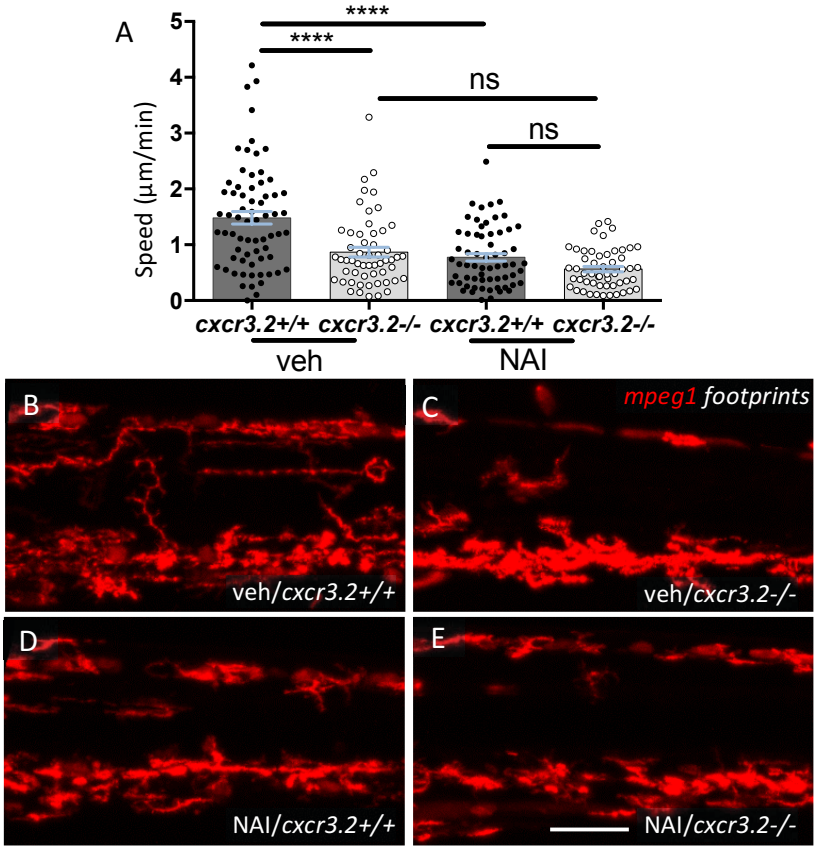

Supplementary Figure 2. Macrophage basal motility requires an active transduction of Nfκb signalling. A. Average speed of wt and mutant macrophage movement after 1 h treatment with 100 nM Nfkb activation inhibitor (NAI) or vehicle (veh); **B-E.** Representative macrophage footprints in wt and mutant embryos treated with Nfκb activation inhibitor or vehicle during the time of observations. Scale bar: 100 µm. Mutant and wt siblings expressing *Tg(mpeg1:mCherry-F)* were imaged at 3 dpf in the trunk area. Data derive from 2 cumulated experiments, run with 3 mutants and 3 wt each.

HYPERLINK TO SUPPLEMENTARY MOVIES

Supplementary Movies are available online at the following URL:
https://drive.google.com/open?id=0B_188Sfgn4xoUkRVNjNKdlNhSEE

REFERENCES

1 Griffith JW, Sokol CL, Luster AD. Chemokines and chemokine receptors: positioning cells for host defense and immunity. Annu Rev Immunol. 2014;32:659-702.
2 Stachowiak AN, Wang Y, Huang YC, Irvine DJ. Homeostatic lymphoid chemokines synergize with adhesion ligands to trigger T and B lymphocyte chemokinesis. J Immunol. 2006 Aug 15;177(4):2340-8.
3 del Pozo MA, Sánchez-Mateos P, Nieto M, Sánchez-Madrid F. Chemokines regulate cellular polarization and adhesion receptor redistribution during lymphocyte interaction with endothelium and extracellular matrix. Involvement of cAMP signaling pathway. J Cell Biol. 1995 Oct;131(2):495-508.
4 Campello S, Lacalle RA, Bettella M, Mañes S, Scorrano L, Viola A. Orchestration of lymphocyte chemotaxis by mitochondrial dynamics. J Exp Med. 2006 Dec 25;203(13):2879-86.

5 Colvin RA, Means TK, Diefenbach TJ, Moita LF, Friday RP, Sever S, Campanella GS, Abrazinski T, Manice LA, Moita C, Andrews NW, Wu D, Hacohen N, Luster AD. Synaptotagmin-mediated vesicle fusion regulates cell migration. Nat Immunol. 2010 Jun;11(6):495-502.
6 Xu Q, Li R, Monte MM, Jiang Y, Nie P, Holland JW, Secombes CJ, Wang T. Sequence and expression analysis of rainbow trout CXCR2, CXCR3a and CXCR3b aids interpretation of lineage-specific conversion, loss and expansion of these receptors during vertebrate evolution. Dev Comp Immunol. 2014 Aug;45(2):201-13.
7 Bajoghli B. Evolution and function of chemokine receptors in the immune system of lower vertebrates. Eur J Immunol. 2013 Jul;43(7):1686-92.
8 Kakuta Y, Okumi M, Miyagawa S, Tsutahara K, Abe T, Yazawa K, Matsunami K, Otsuka H, Takahara S, Nonomura N. Blocking of CCR5 and CXCR3 suppresses the infiltration of macrophages in acute renal allograft rejection. Transplantation. 2012 Jan 15;93(1):24-31.
9 Cuenca AG, Wynn JL, Kelly-Scumpia KM, Scumpia PO, Vila L, Delano MJ, Mathews CE, Wallet SM, Reeves WH, Behrns KE, Nacionales DC, Efron PA, Kunkel SL, Moldawer LL. Critical role for CXC ligand 10/CXC receptor 3 signaling in the murine neonatal response to sepsis. Infect Immun. 2011 Jul;79(7):2746-54.
10 Torraca V, Cui C, Boland R, Bebelman JP, van der Sar AM, Smit MJ, Siderius M, Spaink HP, Meijer AH. The CXCR3-CXCL11 signaling axis mediates macrophage recruitment and dissemination of mycobacterial infection. Dis Model Mech. 2015 Mar;8(3):253-69.
11 Chadzinska M, Golbach L, Pijanowski L, Scheer M, Verburg-van Kemenade BM. Characterization and expression analysis of an interferon-γ2 induced chemokine receptor CXCR3 in common carp (Cyprinus carpio L.). Dev Comp Immunol. 2014 Nov;47(1):68-76.
12 Zhou J, Tang PC, Qin L, Gayed PM, Li W, Skokos EA, Kyriakides TR, Pober JS, Tellides G. CXCR3-dependent accumulation and activation of perivascular macrophages is necessary for homeostatic arterial remodeling to hemodynamic stresses. J Exp Med. 2010 Aug 30;207(9):1951-66.
13 Oghumu S, Varikuti S, Terrazas C, Kotov D, Nasser MW, Powell CA, Ganju RK, Satoskar AR. CXCR3 deficiency enhances tumor progression by promoting macrophage M2 polarization in a murine breast cancer model. Immunology. 2014 Sep;143(1):109-19.
14 Krauthausen M, Kummer MP, Zimmermann J, Reyes-Irisarri E, Terwel D, Bulic B,Heneka MT, Müller M. CXCR3 promotes plaque formation and behavioral deficits in an Alzheimer's disease model. J Clin Invest. 2015 Jan;125(1):365-78.
15 Zhang X, Han J, Man K, Li X, Du J, Chu ES, Go MY, Sung JJ, Yu J. CXC chemokine, receptor 3 promotes steatohepatitis in mice through mediating inflammatory cytokines, macrophages and autophagy. J Hepatol. 2016 Jan;64(1):160-70.
16 Shen K, Sidik H, Talbot WS. The Rag-Ragulator Complex Regulates Lysosome Function and Phagocytic Flux in Microglia. Cell Rep. 2016 Jan 26;14(3):547-59.
17 Torraca V, Masud S, Spaink HP, Meijer AH. Macrophage-pathogen interactions in infectious diseases: new therapeutic insights from the zebrafish host model. Dis Model Mech. 2014 Jul;7(7):785-97.
18 Meijer AH. Protection and pathology in TB: learning from the zebrafish model. Semin Immunopathol. 2015 Sep 1.
19 Ramakrishnan L. The zebrafish guide to tuberculosis immunity and treatment. Cold Spring Harb Symp Quant Biol. 2013;78:179-92.
20 Cronan MR, Tobin DM. Fit for consumption: zebrafish as a model for tuberculosis. Dis Model Mech. 2014 Jul;7(7):777-84.
21 Cosma CL, Klein K, Kim R, Beery D, Ramakrishnan L. Mycobacterium marinum Erp is a virulence determinant required for cell wall integrity and intracellular survival. Infect Immun. 2006 Jun;74(6):3125-33.
22 Takaki K, Davis JM, Winglee K, Ramakrishnan L. Evaluation of the pathogenesis and treatment of Mycobacterium marinum infection in zebrafish. Nat Protoc. 2013 Jun;8(6):1114-24.
23 Roca FJ, Ramakrishnan L. TNF dually mediates resistance and susceptibility to mycobacteria via mitochondrial reactive oxygen species. Cell. 2013 Apr 25;153(3):521-34.
24 Majlessi L, Brodin P, Brosch R, Rojas MJ, Khun H, Huerre M, Cole ST, Leclerc C. Influence of ESAT-6 secretion system 1 (RD1) of Mycobacterium tuberculosis on the interaction between mycobacteria and the host immune system. J Immunol. 2005 Mar 15;174(6):3570-9.
25 van der Vaart M, Spaink HP, Meijer AH. Pathogen recognition and activation of the innate immune response in zebrafish. Adv Hematol. 2012;2012:159807.
26 Chen SC, de Groot M, Kinsley D, Laverty M, McClanahan T, Arreaza M, Gustafson EL, Teunissen MB, de Rie MA, Fine JS, Kraan M. Expression of chemokine receptor CXCR3 by lymphocytes and plasmacytoid dendritic cells in human psoriatic lesions. Arch Dermatol Res. 2010 Mar;302(2):113-23.
27 Kohrgruber N, Gröger M, Meraner P, Kriehuber E, Petzelbauer P, Brandt S, Stingl G, Rot A, Maurer D. Plasmacytoid dendritic cell recruitment by immobilized CXCR3 ligands. J Immunol. 2004 Dec 1;173(11):6592-602.

28 Wang T, Hanington PC, Belosevic M, Secombes CJ. Two macrophage colony-stimulating factor genes exist in fish that differ in gene organization and are differentially expressed. J Immunol. 2008 Sep 1;181(5):3310-22.
29 Wittamer V, Bertrand JY, Gutschow PW, Traver D. Characterization of the mononuclear phagocyte system in zebrafish. Blood. 2011 Jun 30;117(26):7126-35.
30 Zakrzewska A, Cui C, Stockhammer OW, Benard EL, Spaink HP, Meijer AH. Macrophage-specific gene functions in Spi1-directed innate immunity. Blood. 2010 Jul 22;116(3):e1-11.
31 Bergsbaken T, Fink SL, den Hartigh AB, Loomis WP, Cookson BT. Coordinated host responses during pyroptosis: caspase-1-dependent lysosome exocytosis and inflammatory cytokine maturation. J Immunol. 2011 Sep 1;187(5):2748-54.
32 Reddy A, Caler EV, Andrews NW. Plasma membrane repair is mediated by Ca(2+)-regulated exocytosis of lysosomes. Cell. 2001 Jul 27;106(2):157-69.
33 Koo IC, Wang C, Raghavan S, Morisaki JH, Cox JS, Brown EJ. ESX-1-dependent cytolysis in lysosome secretion and inflammasome activation during mycobacterial infection. Cell Microbiol. 2008 Sep;10(9):1866-78.
34 Settembre C, Fraldi A, Medina DL, Ballabio A. Signals from the lysosome: a control centre for cellular clearance and energy metabolism. Nat Rev Mol Cell Biol. 2013 May;14(5):283-96.
35 Sardiello M, Palmieri M, di Ronza A, Medina DL, Valenza M, Gennarino VA, Di Malta C, Donaudy F, Embrione V, Polishchuk RS, Banfi S, Parenti G, Cattaneo E, Ballabio A. A gene network regulating lysosomal biogenesis and function. Science. 2009 Jul 24;325(5939):473-7.
36 Medina DL, Fraldi A, Bouche V, Annunziata F, Mansueto G, Spampanato C, Puri C,Pignata A, Martina JA, Sardiello M, Palmieri M, Polishchuk R, Puertollano R, Ballabio A. Transcriptional activation of lysosomal exocytosis promotes cellular clearance. Dev Cell. 2011 Sep 13;21(3):421-30.
37 Palmieri M, Impey S, Kang H, di Ronza A, Pelz C, Sardiello M, Ballabio A. Characterization of the CLEAR network reveals an integrated control of cellular clearance pathways. Hum Mol Genet. 2011 Oct 1;20(19):3852-66.
38 Pan J, Sun ZY, Ji C, Ji YM, Yang Y, Yang HL. A case of unusual association of Gaucher's disease with spinal tuberculosis. Int J Rheum Dis. 2013 Jun;16(3):361-3.
39 Pérez-Calvo J, Bernal M, Giraldo P, Torralba MA, Civeira F, Giralt M, Pocovi M. Co-morbidity in Gaucher's disease results of a nationwide enquiry in Spain. Eur J Med Res. 2000 Jun 20;5(6):231-5.
40 Liel Y, Rudich A, Nagauker-Shriker O, Yermiyahu T, Levy R. Monocyte dysfunction in patients with Gaucher disease: evidence for interference of glucocerebroside with superoxide generation. Blood. 1994 May 1;83(9):2646-53.
41 Berg RD, Levitte S, O'Sullivan MP, O'Leary SM, Cambier CJ, Cameron J, Takaki KK, Moens CB, Tobin DM, Keane J, Ramakrishnan L. Lysosomal Disorders Drive Susceptibility to Tuberculosis by Compromising Macrophage Migration. Cell. 2016 Mar 24;165(1):139-52.
42 Shen K, Sidik H, Talbot WS. The Rag-Ragulator Complex Regulates Lysosome Function and Phagocytic Flux in Microglia. Cell Rep. 2016 Jan 26;14(3):547-59.
43 Bernut A, Herrmann JL, Kissa K, Dubremetz JF, Gaillard JL, Lutfalla G, Kremer L. Mycobacterium abscessus cording prevents phagocytosis and promotes abscess formation. Proc Natl Acad Sci U S A. 2014 Mar 11;111(10):E943-52.
44 Rougeot J, Zakrzewska A, Kanwal Z, Jansen HJ, Spaink HP, Meijer AH. RNA sequencing of FACS-sorted immune cell populations from zebrafish infection models to identify cell specific responses to intracellular pathogens. Methods Mol Biol. 2014;1197:261-74.
45 Love MI, Huber W, Anders S. Moderated estimation of fold change and dispersion for RNA-seq data with DESeq2. Genome Biol. 2014;15(12):550.
46 Huang da W, Sherman BT, Lempicki RA. Systematic and integrative analysis of large gene lists using DAVID bioinformatics resources. Nat Protoc. 2009;4(1):44-57.
47 Reimand J, Arak T, Vilo J. g:Profiler--a web server for functional interpretation of gene lists (2011 update). Nucleic Acids Res. 2011 Jul;39(Web Server issue):W307-15.
48 van der Sar AM, Abdallah AM, Sparrius M, Reinders E, Vandenbroucke-Grauls CM, Bitter W. Mycobacterium marinum strains can be divided into two distinct types based on genetic diversity and virulence. Infect Immun. 2004 Nov;72(11):6306-12.